Bio-Hybrid Nanocomposite Coatings from Sonicated Chitosan and Nanoclay

Jari Vartiainen,[1] Mikko Tuominen,[2] Kalle Nättinen[3]

[1]*VTT Technical Research Centre of Finland, P.O. Box 1000, FI-02044 VTT, Finland*
[2]*Paper Converting and Packaging Technology, Tampere University of Technology, P.O. Box 541, FI-33101 Tampere, Finland*
[3]*VTT Technical Research Centre of Finland, P.O. Box 1300, FI-33101 Tampere, Finland*

Received 19 October 2009; accepted 4 December 2009
DOI 10.1002/app.31922
Published online 22 February 2010 in Wiley InterScience (www.interscience.wiley.com).

ABSTRACT: Nanocomposite films and coatings with improved properties were produced from ultrasonic dispersed chitosan and hydrophilic bentonite nanoclay. Bio-hybrid coatings were applied onto argon–plasma-activated LDPE coated paper. The intercalation of chitosan in the silicate layers was confirmed by the decrease of diffraction angles as the chitosan/nanoclay ratio increased. Nanocomposite films and multilayer coatings had improved barrier properties against oxygen, water vapor, grease, and UV-light transmission. Oxygen transmission was significantly reduced under all humidity conditions. In dry conditions, over 99% reduction and at 80% relative humidity almost 75% reduction in oxygen transmission rates was obtained. Hydrophilic chitosan was lacking the capability of preventing water vapor transmission, thus total barrier effect of nanoclay containing films was not more than 15% as compared with pure chitosan. Because to very thin coatings ($\leq$1 μm), nanoclay containing chitosan did not have antimicrobial activity against test strains. All coating raw materials were "generally recognized as safe" (GRAS) and the calculated total migration was in all cases $\leq$6 mg/dm^2, thus the coatings met the requirements set by the packaging legislation. Processing of the developed bio-hybrid nanocomposite coated materials was safe as the amounts of released particles under rubbing conditions were comparable with the particle concentrations in a normal office environment.
 J Appl Polym Sci 116: 3638–3647, 2010

Key words: nanocomposites; barrier; biopolymers; clay; coatings

INTRODUCTION

In recent years, a lot of effort has been aimed at developing new nanocomposite barrier packaging materials for foods. Bio-based polymers typically used for the preparation of nanocomposites are polylactide (PLA), poly(3-hydroxy butyrate) (PHB), and its copolymers, thermoplastic starch, plant oils, cellulose, gelatine, and chitosan.[1] Barrier materials against oxygen, water vapor, grease, and light transmission are needed to protect the foods from loosing their physiological (e.g., respiration of fruits), physical (e.g., desiccation, softening, dripping), and chemical (e.g., oxidation of lipids, pigments, vitamins) properties and to extend shelf life or to improve sensory properties, as maintaining the quality of the food. Among the potential fillers for nanocomposites, clay platelets have attracted a particular interest due to their high performance at low filler loadings, rich intercalation chemistry, high surface area, high strength and stiffness, high aspect ratio of individual platelets, abundance in nature, and low cost.[2] Clays are naturally occurring materials composed primarily of fine-grained minerals. Nanoclays (or nanolayered silicates) such as hectorite, saponite, and montmorillonite are promising materials with high aspect ratio and surface area.[3–5] Because of their unique platelet-like structure nanoclays have been widely studied as regards the barrier properties. Such nanoclays can be very effective at increasing the tortuosity of the diffusion path of the diffusing molecules, thus significant improvement in barrier properties can be achieved with the addition of relatively small amounts of clays.[6] When the nanoclay layers are completely and uniformly dispersed in a continuous polymer matrix, an exfoliated or delaminated structure is obtained. Full exfoliation (single platelet dispersion) of nanoclay by using existing/traditional compounding techniques is very difficult due to the large lateral dimensions of the layers, high intrinsic viscosity of the polymer, and a strong tendency of clay platelets to agglomerate.[7–9] Most of the clays are hydrophilic, thus mixing in water with water-soluble polymers results good dispersion, especially when the sufficient amount of

Correspondence to: J. Vartiainen (jari.vartiainen@vtt.fi).
Contract grant sponsor: Tekes (Finnish Funding Agency for Technology and Innovation); contract grant number: 40409/05.
Contract grant sponsor: VTT Technical Research Centre of Finland.

mixing energy is used. The degree of exfoliation can be improved by the use of conventional shear devices such as extruders, mixers, ultrasonicators, ball milling, fluidizators, etc. Chitosan is a polysaccharide prepared by the *N*-deacetylation of chitin, the second most abundant natural biopolymer after cellulose. Chitosan is an edible and biodegradable material that also has antimicrobial activity against different groups of microorganisms, including bacteria, yeasts, and molds. The activity of chitosan is mainly based on its amino groups, which are positively charged below pH 6. As chitosan is both hydrophilic and cationic in acidic conditions, it has usually good miscibility with negatively charged nanoclays. Chitosan chains may easily intercalate into the clay interlayer by means of cationic exchange.[10] In addition, nanoclays treated with chitosan have provided better interaction between clays and other matrixes.[11] Chitosan/layered silicate nanocomposites have been used to improve both barrier, mechanical and antimicrobial properties.[12–17] The extended use of waste sidestream of agriculture and the food industry will be of particular value in the future. Bio-based nanocomposites are entirely new types of materials based on plant and natural materials (organoclay). During composting, they are safely decomposed into CO_2, water, and humus through the activity of microorganisms. Thus, bio-based nanocomposites have tremendous market potential both as replacements for current synthetic composites and in the creation of new markets through their unique properties.[7]

MATERIALS AND METHODS

Chitosan was obtained from Fluka BioChemika (low-viscous with a molecular weight of 150 kDa) and hydrophilic bentonite nanoclay (Nanomer PGV) from Aldrich. According to manufacturer, nanoclay was untreated (no organic modification) hydrophilic clay (>98% montmorillonite) with aspect ratio of 150–200. Acetic acid (99.8%) was from Riedel–de Haën. Low-density polyethylene (LDPE; CA 7230) was obtained from Borealis and Lumiflex pigment-coated paper (90 g/m^2) from Stora Enso.

Extrusion coating and plasma activation

LDPE (17 g/m^2) was extrusion coated onto paper at the pilot line of Tampere University of Technology (TUT)/Paper Converting and Packaging Technology (PCT). Atmospheric plasma treatment was used to activate the surface of the LDPE coated paper. The atmospheric plasma treatment (APT) unit operates continuously (roll-to-roll) at normal air atmosphere. The atmospheric plasma was generated using a dielectric barrier discharge. The feed rate of plasma gas, that is, argon was 30 L/min, the line speed was 25 m/min, the treatment width was 380 mm, and the treatment efficiency was 84.2 W min m^{-2}.

Preparation of nanocomposite films and coatings

Nanoclay (0.2, 1, and 2 wt %) was swelled in 30 mL of distilled water and dispersed using ultrasonification tip (Branson Digital Sonifier) for 10 min. The dispersion was added into 30 mL of 1% chitosan in 1% acetic acid, followed by sonication for 10 min. For reducing the surface tension and increasing the wettability, 60 mL of ethanol was added and mixed under rigorous mixing. For self-standing films, 15 mL of each solution was cast onto polystyrene Petri dish (Ø 8.5 cm) and dried at room temperature. The obtained films were peeled from the Petri dishes and stored at room temperature, and 50% relative humidity before tests. Nanocomposite chitosan films had initial nanoclay concentrations of 0, 17, 50, and 67 wt %, and total film dry weight of 5–15 g/m^2.

For coated multilayer structures, the solutions were applied onto plasma-activated LDPE coated paper using the standard coating bar no. 6 (wet film deposit of 60 μm). Chitosan solutions with initial nanoclay concentrations of 0, 17, 50, and 67 wt %, and total coating dry weight of 0.2–0.6 g/m^2 were used. Coated samples were dried for 3 h at room temperature, and stored at room temperature and 50% relative humidity before tests.

Scanning electron microscopy (SEM)

Structures of pure nanoclay in sonicated dispersions were analyzed using scanning electron microscopy (SEM, LEO DSM 982 Gemini FEG-SEM). SEM samples of aqueous dispersions of pure nanoclay were prepared by spreading dispersions on a polyvinyl amine premodified silica surface using fast spinning (2800 rpm for 1 min). Typically, no conductive coating was applied on the specimen prior SEM imaging. However, in some cases a thin layer (~ 10 nm) of platinum was sputter coated on the surface to improve conductivity and stability of the specimen. The SEM analyses of the aqueous dispersions were conducted using electron energies of 1.0 kV and 2.0 kV. JEOL JSM-6360LV with accelerating voltage control of 10 kV was used to investigate the cross-section and surface topography of coated multilayer structures.

X-ray diffraction

X-ray diffraction (XRD) was used to determine the interlayer distance of layered nanoclays and chitosan nanocomposites. Interlayer distances were calculated by the Bragg's equation: $2d \sin \theta = \lambda$, where d is the interlayer distance, 2θ is the diffraction angle, and λ

is the wavelength of the X-ray ($\lambda = 1.542$ Å). X-ray diffractograms were run from the samples using Philips X'Pert MPD diffractometer, powder method, and Cu X-ray tube.

Profilometry

Wyko NT9100 Optical Profiling System was used to visualize the three-dimensional topography and to determine the roughness average (R_a) of chitosan coatings. R_a is the arithmetic mean of the absolute values of the surface departures from the mean plane. It is a stable, easily implemented parameter, useful for detecting general variations in overall surface height characteristics.

Water contact angle

Water contact angles of the coated surface were measured using CAM200 equipment (KSV Instruments, Finland) in test conditions of 23°C and 50% relative humidity. Contact angle values were measured as a function of time during 2 min.

Light absorption measurements

UV-visible light absorption of the self-standing films between 200 and 800 nm was determined using Shimadzu UV-1800 UV-spectrophotometer.

WVTR

Water vapor transmission rates (WVTR) of self-standing films were determined gravimetrically using a modified ASTME-96 procedure. Samples with a test area of 25 cm^2 were mounted on a circular aluminum dish (H.A. Büchel V/H, A.v.d. Korput, Baarn-Holland 45M-141), which contained distilled water. Dishes were stored in test conditions of 23°C and 50% relative humidity, and weighed periodically until a constant rate of weight reduction was attained. Weighings were used to determine the amount of moisture transferred through the film from the cup toward lower humidity in climate room. The relative humidity difference (the humidity gradient) during the test was 50%.

OTR

Oxygen transmission measurements were performed with Oxygen Permation Analyser Model 8001 (Systech Instruments, UK). The tests were carried out at 23°C and 0, 50, and 80% relative humidity using circular samples with a test area of 5 cm^2 (films) and 50 cm^2 (coated paper).

Grease resistance

Grease resistance was determined according to modified Tappi T 507 method. First, standard olive oil was colored with Sudan II dye and applied onto 5 cm × 5 cm sized blotting paper. Stain saturated piece of blotting paper was placed against self-standing films and a piece of blank blotting paper (stain absorber) was placed against the other side. The whole stack was pressed between two platelets and kept in oven at 60°C for 4 h. At the end of the test period, the assembly was removed and the stain absorbers were examined. For each absorber, the area and the number of stained spots, if any, were determined.

Antimicrobial activity

Antimicrobial activity was determined as described in standard JIS Z 2801: 2000 "Antimicrobial products—test for antimicrobial activity and efficacy." Bacterial suspensions of *Staphylococcus aureus* (8.8×10^5 cfu/mL) and *Escherichia coli* (4.5×10^5 cfu/mL) were placed on the surface of coated samples, covered with a plastic foil and incubated for 24 h at 35°C. After incubation, the bacteria were washed from the samples and the number of viable bacteria was measured by plating. The number of viable bacteria eluted from the antimicrobial samples was compared with that eluted from the reference LDPE coated paper.

Particle release

Test method was developed for testing particle release from planar materials. Particle measurements were performed with Met One R4815 optical particle sensor. Particle sensor counts two particle sizes: 0.5 μm and 5 μm. Particle sensor was attached to a moving nozzle. Nozzle had an automated reciprocating motion, motion length and repetition were computer controlled. When nozzle was moving forward, sample surface was flushed with clean pressurized air and particles were absorbed from the sample surface. When nozzle was moving backward, sample surface was rubbed with the nozzle bottom and particles were absorbed from the sample surface after rubbing. Measurements were performed in the clean room to avoid deposition of normal air particles to the sample surface.

RESULTS AND DISCUSSION

Microstructure

Nanoclay was delivered as dry powder with particle size of 2–15 μm [Fig. 1(a)]. According to manufacturer, the material was composed of high purity

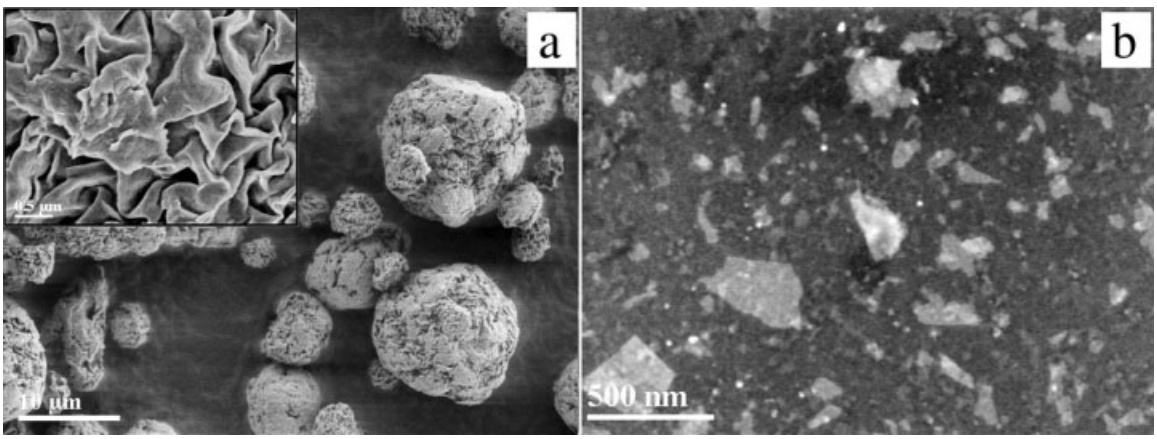

Figure 1 SEM images of (a) typical nanoclay aggregates prior dispergation and (b) spincoated nanoclay platelets after ultrasonic dispergation.

aluminosilicate minerals (98% montmorillonite), intended for use as additive to hydrophilic polymers such as polyvinylalcohols, polysaccharides, and polyacrylic acids. When fully dispersed, the nanoclay was supposed to form nanocomposites with the host polymers.

Nanoclays typically tend to be agglomerated when mixed into water. The agglomerates are held together by attraction forces of various physical and chemical nature, including van der Waals forces and water surface tension. These attraction forces must be overcome in order to deagglomerate and disperse the clays into water. Ultrasonication was used to create sound waves that propagate into water resulting in alternating pressure cycles, which overcome the bonding forces and break the agglomerates.

As can be seen in Figure 1(a), dry nanoclay powder consisted of round particles with coarse and platelety surface. By ultrasonic dispersing, the nanoclay platelets were effectively ripped off and uniformly distributed on the surface. The diameter of the intercalated nanoplatelets varied between 100 and 500 nm [Fig. 1(b)]. Previous studies have demonstrated that nanoclay platelets could be oriented parallel to the surface of especially solution cast coatings.[18,19]

As high viscosity of dispersion may promote agglomeration, the low-viscous grade of chitosan was used. As previously established, sonication may also lead to a scission of chitosan chains and an increase of short chains and oligomers.[20] As a result of depolymerization, the viscosity of dispersion decreases.[21] At the same time, the viscosity at low shear rates tend to increase with clay concentration and especially if agglomerates are reformed.[6]

Addition to adequate viscosity, also surface tension of coating dispersion must be regulated. A total of 50% of ethanol was added to chitosan–nanoclay dispersion for reducing the surface tension, and thus improving the wettability. Extrusion coated LDPE formed an even layer of 18 μm on Lumiflex pigment-coated paper. Argon–plasma activation was used to increase the surface energy of LDPE, which would enable more homogenous and even dispersion coating top layer. Indeed, the dispersions were easily applied onto LDPE coated paper with wet film deposit of 60 μm and dry thickness varying between 0.5 and 1 μm. Pure chitosan formed thinner coatings, whereas coatings with 67 wt % of nanoclay had thicker and rougher surfaces (Fig. 2).

Chitosan was dissolved in 1% acetic acid before contact with nanoclays. Acidic pH was necessary for the protonation of amino groups of chitosan. Positively charged amino groups had two main functions: they provided coulombic interactions with (a) the negative sites in the clay structure facilitating chitosan intercalation into nanoclay interlayer space,[22] and (b) the anionic molecules at the bacteria cell surface resulting in antimicrobial activity.[23]

Intercalated structures are formed when extended chitosan chains are intercalated between the silicate layers. The result is a well-ordered multilayer structure of alternating biopolymeric and inorganic layers with a repeat interlayer distance (*d*-value) between them. The *d*-values were measured by XRD using the Braggs's equation. The pure powdery nanoclay had an interlayer distance of 1.23 nm. By sonication, the *d*-values of 67, 50, and 17 wt % of nanoclay containing chitosan films were increased to 1.47, 1.58, and 1.62 nm, respectively (Fig. 3). Higher nanoclay contents reduced the distance between layers which may have caused a tendency toward aggregation and restacking of nanoplatelets. These findings are consistent with the earlier studies where increasing of montmorillonite content created flocculated structures.[17] As previously established, the thickness of the individual sheet of chitosan chain is 0.38 nm.[24,25] In this case, the diffractograms support the intercalation of chitosan in a monolayer configuration.

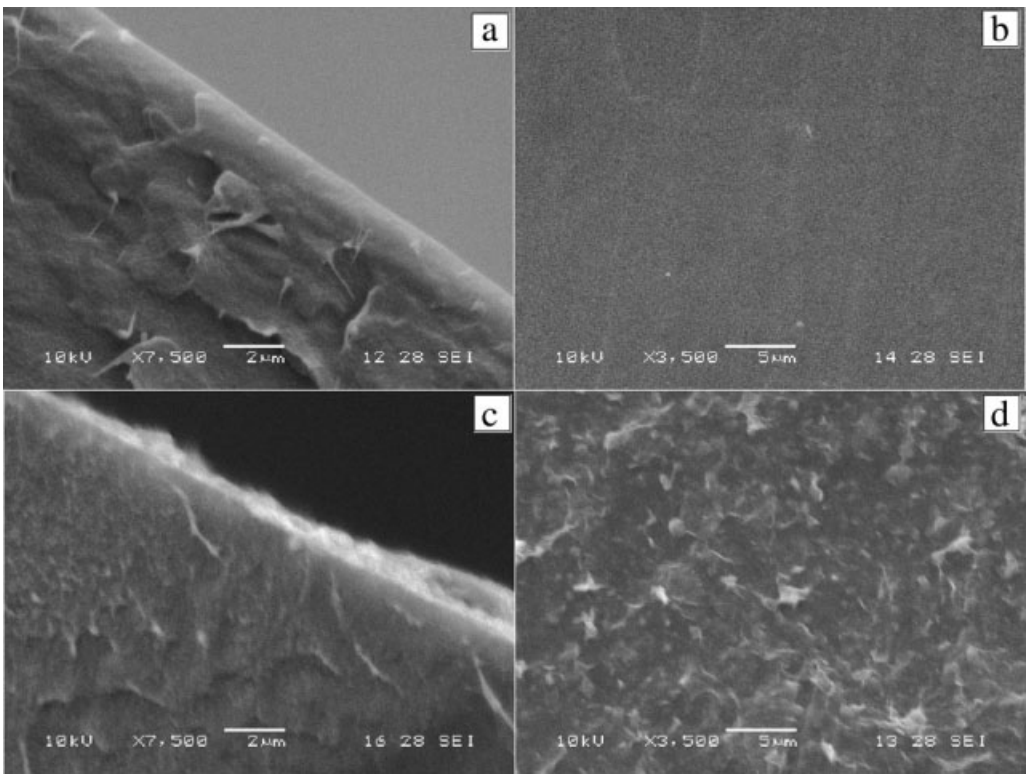

Figure 2 SEM image of cross-section and surface topography of chitosan coatings on plasma-activated LDPE coated paper. Chitosan coatings with 0 wt % (a and b) and 67 wt % (c and d) of nanoclay, respectively.

Monolayer adsorption was mainly controlled by a cationic exchange mechanism due to the coulombic interactions between the positive amino groups of chitosan and the negative sites in the clay structure.[10,26]

Coating properties

As water contact angle measurements indicated, the Argon–plasma activation increased hydrophilicity of LDPE coated paper as was expected. Hydrophilic chitosan coating had even more affinity to moisture. Nanoclays are known as very strong absorbents with capability of absorbing several times their dry mass in water. Indeed, coatings containing 17 and 50 wt % of nanoclay decreased the contact angles without increasing the roughness. Excess amount of nanoclay (67 wt %) increased the roughness, which may also have had additional positive effect on wettability (Fig. 4). The smoothness increased as a function of nanoclay concentration up to 50 wt %. This may be due to clay platelets that were oriented onto surface. As chitosan concentration increased, the continuous structure was vanished and the surface became more network-like.[27] Higher nanoclay concentration (67 wt %) created reagglomeration of platelets, which resulted in increased surface roughness. Regardless of minor variations, the surface roughness was not significantly influenced by the nanoclays as average roughness values (R_a) of all samples remained within 200 nm, which is of the same order of magnitude as the length of single nanoplatelets (Fig. 5).

Light transmission through packaging materials affects the quality of many products inside them. Especially, ultraviolet radiation (300–400 nm) causes photo-oxidation of photosensitive foods, such as meat, beer, and milk resulting in changes in color,

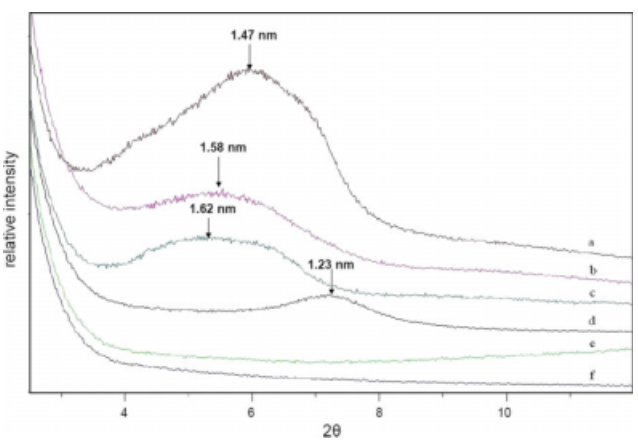

Figure 3 XRD-patterns of chitosan films containing (a) 67 wt %, (b) 50 wt %, (c) 17 wt % of nanoclay, (d) pure powdery nanoclay, (e) chitosan film without nanoclay, and (f) silicon base-line. [Color figure can be viewed in the online issue, which is available at www.interscience.wiley.com.]

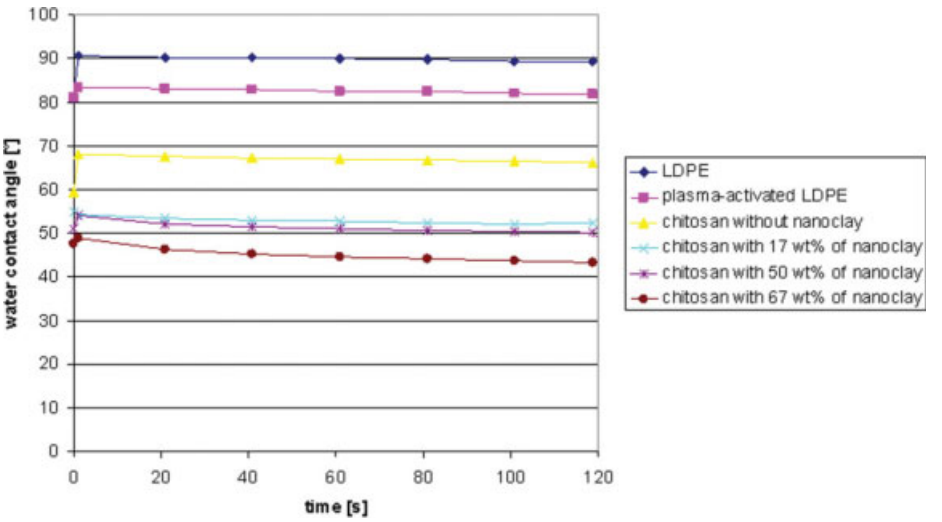

Figure 4 Water contact angles of different coatings. [Color figure can be viewed in the online issue, which is available at www.interscience.wiley.com.]

flavor, and taste. As the packaging materials, in general, should be as transparent as possible, the optimal UV-barrier absorbs the radiation below 400 nm, but not the visible light (400–760 nm).

Chitosan without nanoclays formed completely clear and transparent films. Nanoclay containing films were transparent but slightly opaque. Absorption of irradiation below 300 nm increased as a function of nanoclay concentration. This is not surprising as the separated nanoplatelets had lengths varying between 100 and 500 nm. Especially, higher amounts of nanoclays decreased the transparency in visual wavelengths (Fig. 6). The results are consistent with the earlier findings where no marked decrease was found in the clarity due to the small amounts of well-dispersed nanofillers.[14] The individual nanoclay platelets are $\sim$ 1 nm thick. When single layers are dispersed in a polymer matrix, the resulting nanocomposites are optically clear in the visible region, whereas a loss of intensity in the UV region (for $<$250 nm) is noticed mostly due to scattering by the nanoclay particles.[6] Higher amounts of nanoclays typically have a tendency to agglomerate, which increases the absorption.[14]

As water vapor transmission results indicated, nanoclays slightly improved the barrier properties of self-standing films (Fig. 7). The same behavior was found with starch/clay nanocomposites where the increasing clay content also led to an improvement in barrier properties.[28] In high humidity conditions, nanoclay platelets absorbed water and expanded, but still formed single individual barrier layers against vapor transmission. At the same time, the penetrating water molecules effectively plasticized and swelled the matrix polymer. Hydrophilic chitosan was lacking the capability of preventing water vapor transmission, thus total barrier effect of nanoclay containing films was not more than 15% as compared with pure chitosan. In the case of more hydrophobic PLA nanocomposites, the nanoclay incorporation decreased the water vapor transmission of the resulting films by about 40–50%[29]. Barrier improvements are explained using tortuous path theory, which relates to alignment of the nanoclay platelets. As a result of intercalation, the effective path length for molecular diffusion increases and the path becomes highly tortuous to reduce the effect of gas and moisture transmission through the film.[30]

As the amounts of platelets increased, the barrier properties improved. However, the highest amount of nanoclay (67 wt %) did not further improve the barrier, thus excess amount had no advantage. High amount of nanoclay promoted the agglomeration, which produced surface roughness and inhomogeneity having negative influence on water vapor barrier. This may also be associated with the increased hydrophilic nature of chitosan due to the introduction of excess amount of polar groups from

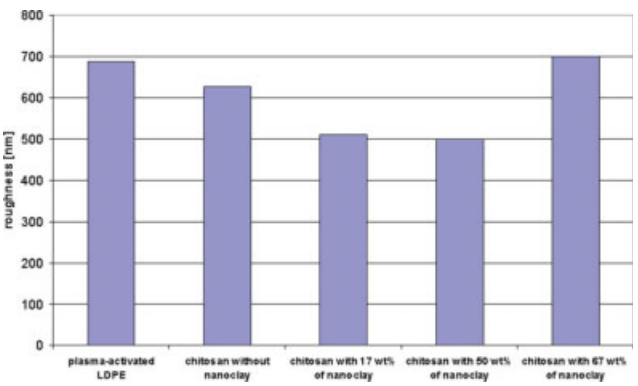

Figure 5 Average roughness (R_a) of different coatings. [Color figure can be viewed in the online issue, which is available at www.interscience.wiley.com.]

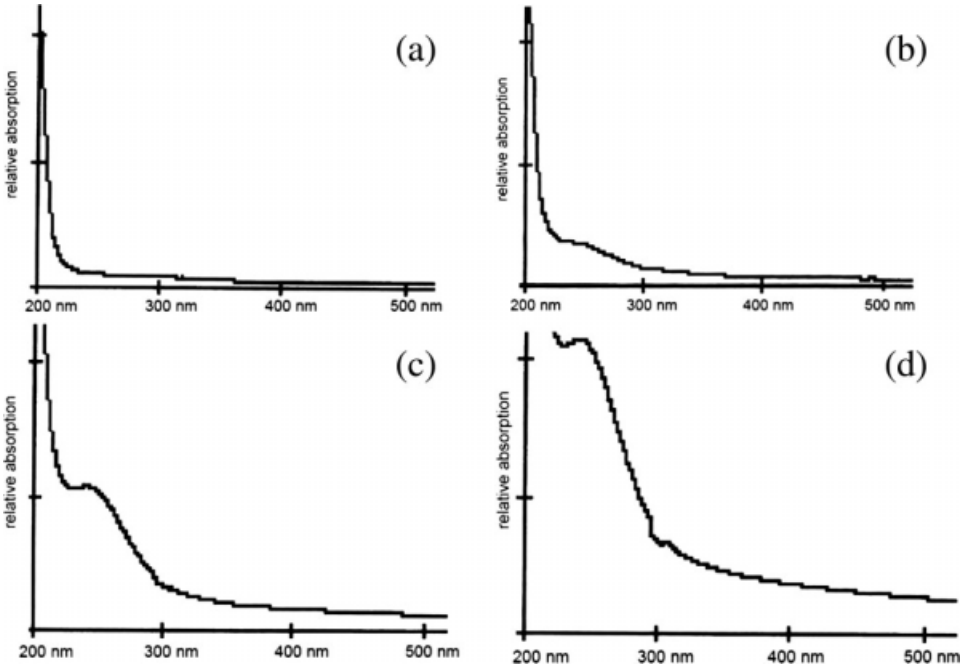

Figure 6 Light absorption of chitosan films containing (a) 0%, (b) 17%, (c) 50%, and (d) 67 wt % of nanoclay.

nanoclay. The absorbed water molecules weaken the intermolecular interactions of chitosan driving to dissolve more water and increasing the water transmission rate, which lead to reduced barrier properties of nanoclay in biopolymer.[13]

Chitosan and other biopolymers with crystalline structure and hydrogen bonds are typically very good oxygen barriers, but only up to 50% relative humidity. In high humidity conditions, water molecules penetrate between chitosan chains and destroy the hydrogen bonded structure and barrier properties. Nanoclays clearly improved the oxygen barrier properties in high humidity conditions (Fig. 8). A total of 88% reduction in transmission was obtained with chitosan films containing 67 wt % of nanoclay. These results are consistent with other studies[31–34] where 15–88% reduction in oxygen transmission rates has been attained with PET- and PLA-based layered silicate nanocomposites.

Nanocomposite coatings applied onto plasma-activated LDPE coated paper, which effectively decreased the oxygen transmission under all humidity conditions (Fig. 9). In dry conditions, over 99% reduction and, at 80% relative humidity, almost 75% reduction in oxygen transmission rates were obtained. Highest concentration of nanoclay (67 wt %) offered the best barrier against oxygen, whereas the 17 wt % concentration of nanoclay performed almost as good as 50 wt % of nanoclay. Interlayer distances with lower amounts of nanoclay were slightly longer, thus tortuous path in that sense would be longer as well. Higher total nanoclay

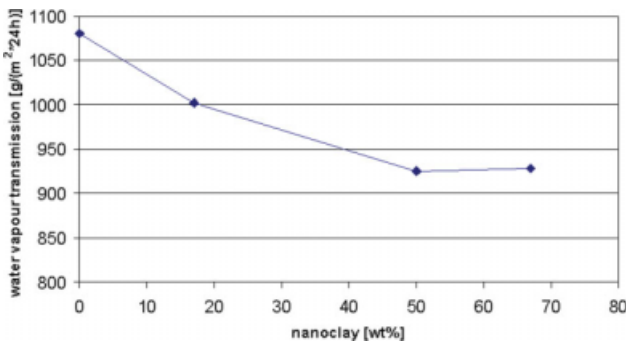

Figure 7 Water vapor transmission of chitosan films with different concentrations of nanoclay. Measurements were carried out at 23°C and 50% relative humidity. [Color figure can be viewed in the online issue, which is available at www.interscience.wiley.com.]

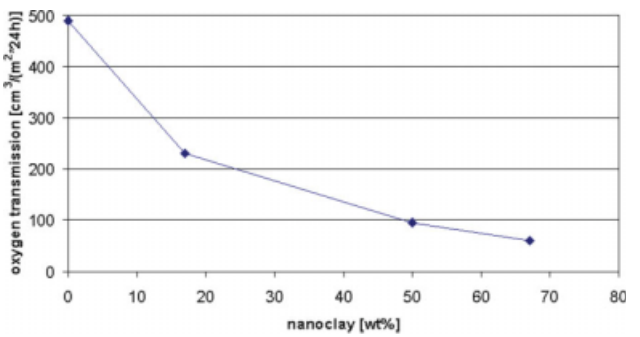

Figure 8 Oxygen transmission of chitosan films with different concentrations of nanoclay. Measurements were carried out at 23°C and 80% relative humidity. [Color figure can be viewed in the online issue, which is available at www.interscience.wiley.com.]

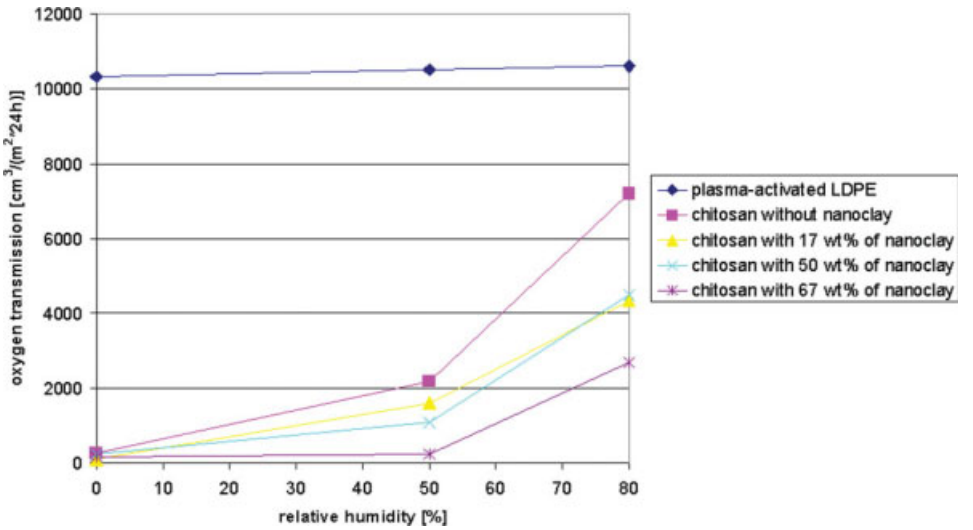

Figure 9 Oxygen transmission of different coatings. Measurements were carried out at 23°C and 0, 50, and 80% relative humidity. [Color figure can be viewed in the online issue, which is available at www.interscience.wiley.com.]

content, on the other hand, provided more impermeable clay material. Barrier effects of nanoclay became less evident in dry conditions. Presumably higher nanoclay concentrations were partly agglomerated, which hindered the crystallization and hydrogen bonding formation between chitosan chains, especially in dry conditions.

Bentonite clay has a capability of adsorbing oils and greases. However, it did not have any effects on grease resistance of self-standing films. The results indicated that all films were totally impermeable to grease under the conditions tested. The results are consistent with earlier studies of fat resistant chitosan-based paper packaging.[35] Hydrogen bonds in chitosan enable excellent barrier properties against grease. In this case, chitosan formed a continuous phase, which totally prevented the penetration.

Antimicrobial properties were determined as described in standard JIS Z 2801. Activity was expressed using *R*-value as follows: $R = \log B - \log C$, where *B* is the viable cells on reference after 24 h and *C* is the viable cells on sample after 24 h. Materials are evaluated as having antimicrobial properties if calculated reduction value of $R \geq 2$ is attained. None of the coatings were effective against Gram-positive *S. aureus* or Gram-negative *E. coli*. After 24 h of incubation, a minor reduction of 0.54 logarithmic units in *S. aureus* cell numbers was observed with pure chitosan coating. Other coatings were inactive (Tables I and II).

Previous studies have demonstrated that chitosan/rectorite nanocomposites have antimicrobial activity against both Gram-positive and Gram-negative bacteria.[12,14] As rectorite has structure and characteristic comparable with montmorillonite, the antimicrobial activity of these both layered silicates should approximately be the same. *In vitro* tests have shown that pristine rectorite could not inhibit the growth of bacteria, but only chitosan/layered silicate nanocomposite had enhanced activity. Typically, the antimicrobial properties of chitosan acetate have two separate mechanisms: (1) Carboxylate groups in the form of evaporated acid residues and (2) diffused protonated glucosamine fractions.[36] Positively charged amino groups interact with the outer membranes of microorganisms causing the death of the microbial

TABLE I
Antimicrobial Activity Against *S. aureus* Expressed as $R = \text{Log } B - \text{Log } C$

Chitosan coating	*B* (cfu/cm^2)	*C* (cfu/cm^2)	Log *B*	Log *C*	*R*
Nanoclay 0 wt %	1.11×10^5	3.20×10^4	5.05	4.51	0.54
Nanoclay 17 wt %	1.11×10^5	3.17×10^5	5.05	5.50	−0.45
Nanoclay 50 wt %	1.11×10^5	2.57×10^5	5.05	5.41	−0.36
Nanoclay 67 wt %	1.11×10^5	2.48×10^5	5.05	5.40	−0.35

TABLE II
Antimicrobial Activity Against *E. coli* Expressed as $R = \text{Log } B - \text{Log } C$

Chitosan coating	*B* (cfu/cm^2)	*C* (cfu/cm^2)	Log *B*	Log *C*	*R*
Nanoclay 0 wt %	6.08×10^6	1.06×10^7	6.78	7.02	−0.24
Nanoclay 17 wt %	6.08×10^6	5.96×10^6	6.78	6.77	0.01
Nanoclay 50 wt %	6.08×10^6	9.25×10^6	6.78	6.97	−0.19
Nanoclay 67 wt %	6.08×10^6	9.37×10^6	6.78	6.97	−0.19

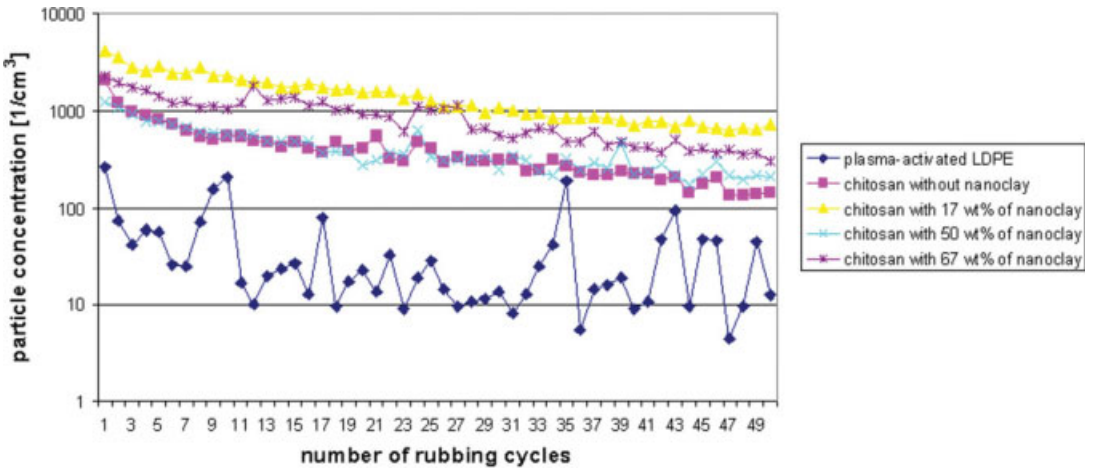

Figure 10 Particle concentration of 0.5-μm sized particles in air during rubbing of different coatings. [Color figure can be viewed in the online issue, which is available at www.interscience.wiley.com.]

cell.[23] Although the nanoclay itself does not have antimicrobial activity, it may adsorb the bacteria from the solution enabling better interaction with chitosan.[12] The previous antimicrobial tests with chitosan/rectorite nanocomposites were carried out using either buffer solutions at a concentration of 1% (w/v)[12] or 30 μm films in shake-flasks (tubes)[14] during continuous agitation at 37°C for 24 h. Antimicrobial test method (JIS Z 2801) used in this study is designed to film shaped materials with intimate but static contact with microbial organisms. As coating thicknesses in this case varied between 0.5 and 1 μm, the total exposure of test strain to antimicrobial coating was significantly lower as compared with previous studies. It is the reason to believe that antimicrobial properties of chitosan/montmorillonite nanocomposites are comparable with chitosan/rectorite if tested with similar methods and concentrations.

Safety aspects of nanomaterials have recently raised many concerns. Both chitosan and bentonite clay have been approved for use as "generally recognized as safe" (GRAS) food additives in the USA. Bentonite has also a food additive code number E558 meaning, it is approved for use in the European Union. The overall migration limit for the total amount of substances migrating from the packaging material into the food is stipulated in Directive 2002/72/EC. The limit value is 60 mg/kg of packed food or 10 mg/dm^2 of packaging material. Biohybride coatings developed in this study meet the requirements set by the food packaging legislation, as total amount of raw materials including chitosan and nanoclay remain in all cases $\leq$6 mg/dm^2.

The lungs are the primary route of entry of nanoparticles into the human body. Inhalation of nanoparticles may occur as a consequence of their release into the environment, either during their

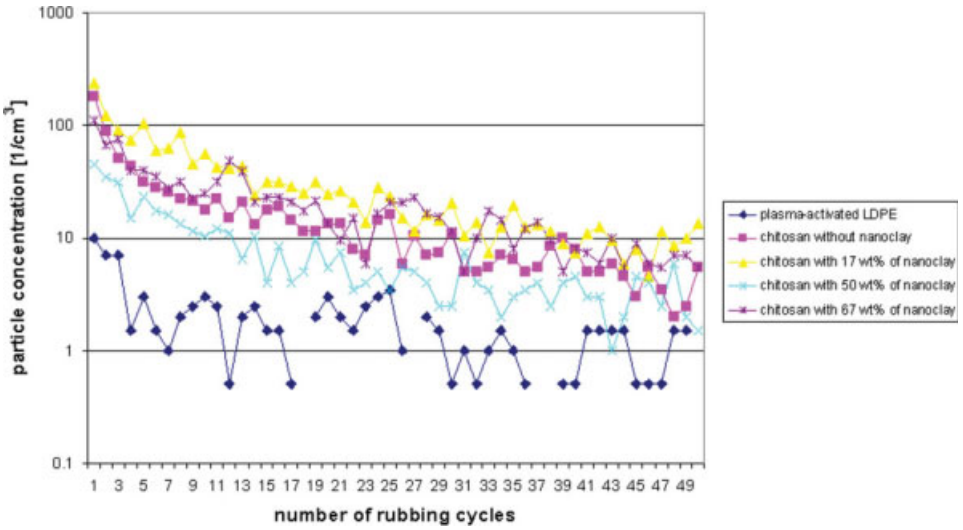

Figure 11 Particle concentration of 5-μm sized particles in air during rubbing of different coatings. [Color figure can be viewed in the online issue, which is available at www.interscience.wiley.com.]

manufacture or utilization.[37] There is some evidence that long-term occupational exposure to bentonite dust may cause structural and functional damage to the lungs.[38] Also inhaled chitosan microparticles especially in high concentrations can have pro-inflammatory effects on lung tissues.[39]

As particle measurements indicated the amounts of released particles under rubbing conditions were really low. Amounts of 5-μm and 0.5-μm sized particles were below 100 and 10,000 particles/cm^3, respectively (Figs. 10 and 11). The air in a normal office room typically contains 10,000–20,000 nanoparticles/cm^3, whereas the concentration in urban streets can be as high as 100,000 nanoparticles/cm^3. As expected, the biohybride coatings increased the amounts of released particles as compared with reference LDPE coated paper. However, there were only minor differences between pure chitosan coatings and coatings containing nanoclay. Thus, it seems that chitosan formed an effective binder matrix around both agglomerated nanoclays and intercalated nanoclay sheets.

CONCLUSIONS

There is increasing interest in barrier packaging materials, which utilize bio-based components or layers. Hydrophilic bentonite nanoclay was successfully dispersed in aqueous chitosan solution using ultrasonic mixing. The intercalation of chitosan in the silicate layers was confirmed by the decrease of diffraction angles, whereas the chitosan/nanoclay ratio increased. Nanocomposite films and multilayer coatings had improved barrier properties against oxygen, water vapor, grease, and UV-light transmission. The developed nanocomposite films and coatings can be potentially exploited as safe and environmentally sound alternatives for synthetic barrier packaging materials.

The authors thank Pirjo Hakkarainen, Heli Nykänen, Mari Leino, Juha Hokkanen, Unto Tapper, Marjaana Rättö, Tapio Kalliohaka, Sirpa Vapaavuori, and Mirja Nygård for their technical help. They also thank all project partners as well as Tekes (the Finnish Funding Agency for Technology and Innovation) and VTT Technical Research Centre of Finland for funding this study (funding decision 40409/05). The work was carried out within Plastek-project "Surface Modification with Plasma and Corona Techniques."

References

1. Romero, R. B.; Leite, C. A. P.; Gonçalves, M. Polymer 2009, 50, 161.
2. Blumstein, A. J Polym Sci Part A: Gen Pap 1965, 3, 2653.
3. Lan, T.; Kaviratna, P. D.; Pinnavaia, T. J. Chem Mater 1994, 6, 573.
4. Messersmith, P. B.; Giannelis, E. P. J Polym Sci Part A: Polym Chem 1995, 33, 1047.
5. Yano, K.; Usuki, A.; Okada, A. J Polym Sci Part A: Polym Chem 1997, 35, 2289.
6. Pavlidou, S.; Papaspyrides, C. D. Prog Polym Sci 2008, 33, 1119.
7. Hussain, F.; Hojjati, M.; Okamoto, M.; Gorga, R. E. J Compos Mater 2006, 40, 1511.
8. Ericson, L. M. Masters Thesis, Rice University, 2000.
9. Jana, S. C.; Jain, S. Polymer 2001, 42, 6897.
10. Depan, D.; Kumar, B.; Singh, R. P. J Biomed Mater Res B 2008, 84, 184.
11. Wu, T.-M.; Wu, C.-Y. Polym Degrad Stab 2006, 91, 2198.
12. Wang, X.; Du, Y.; Yang, J.; Wang, X.; Shi, X.; Hu, Y. Polymer 2006, 47, 6738.
13. Tang, C.; Chen, N.; Zhang, Q.; Wang, K.; Fu, Q.; Zhang, X. Polym Degrad Stab 2009, 94, 124.
14. Wang, X.; Du, Y.; Luo, J.; Lin, B.; Kennedy, J. F. Carbohydr Polym 2007, 69, 41.
15. Xu, Y.; Ren, X.; Hanna, M. A. J Appl Polym Sci 2006, 99, 1684.
16. Lin, K.-F.; Hsu, C.-Y.; Huang, T.-S.; Chiu, W.-Y.; Lee, Y.-H.; Young, T.-H. J Appl Polym Sci 2005, 98, 2042.
17. Wang, S. F.; Shen, L.; Tong, Y. J.; Chen, L.; Phang, I. Y.; Lim, P. Q.; Liu, T. X. Polym Degrad Stab 2005, 90, 123.
18. Malwitz, M. M.; Lin-Gibson, S.; Hobble, E. K.; Butler, P. D.; Schmidt, G. J Polym Sci Part B: Polym Phys 2003, 41, 3237.
19. Ogata, N.; Jimenez, G.; Kawai, H.; Ogihara, T. J Polym Sci Part B: Polym Phys 1997, 35, 389.
20. Popa-Nita, S.; Lucas, J.-M.; Ladavie'Re, C.; David, L.; Domard, A. Biomacromolecules 2009, 10, 1203.
21. No, H. K.; Nah, J. W.; Meyers, S. P. J Appl Polym Sci 2003, 87, 1890.
22. Pan, J. R.; Huang, C.; Chen, S.; Chung, Y. C. Colloids Surf A 1999, 147, 359.
23. Helander, I. M.; Nurmiaho-Lassila, E.-L.; Ahvenainen, R.; Rhoades, J.; Roller, S. Int J Food Microbiol 2001, 71, 235.
24. Clark, G. L.; Smith, A. F. J Phys Chem 1936, 40, 863.
25. Darder, M.; Colilla, M.; Ruiz-Hitzky, E. Chem Mater 2003, 15, 3774.
26. Darder, M.; Colilla, M.; Ruiz-Hitzky, E. Appl Clay Sci 2005, 28, 199.
27. Liang, S.; Liu, L.; Huang, Q.; Yam, K. T. J Phys Chem B 2009, 113, 5823.
28. Park, H. M.; Lee, W. K.; Park, C. Y.; Cho, W. J.; Ha, C. S. J Mater Sci 2003, 38, 909.
29. Thellen, C.; Orroth, C.; Froio, D.; Ziegler, D.; Lucciarini, J.; Farrell, R.; D'souza, N. A.; Ratto, J. A. Polymer 2005, 46, 11716.
30. Christopher, O. O.; Lerner, M. Nanocomposites and Intercalation Compound, Encyclopedia of Physical Science and Technology, 3rd ed.; Academic Press: San Diego, California, 2001; Vol. 10.
31. Ke, Z.; Yongping, B. Mater Lett 2005, 59, 3348.
32. Lange, J.; Wyser, Y. Packag Technol Sci 2003, 16, 149.
33. Ray, S. S.; Yamada, K.; Okamoto, M.; Ueda, K. Polymer 2003, 44, 857.
34. Chang, J.-H.; Uk-An, Y.; Sur, G. S. J Polym Sci Part B: Polym Phys 2003, 41, 94.
35. Ham-Pichavant, F.; Sebe, G.; Pardon, P.; Coma, V. Carbohydr Polym 2005, 61, 259.
36. Lagaron, J. M.; Fernandez-Saiz, P.; Ocio, M. J. J Agric Food Chem 2007, 55, 2554.
37. NIOSH. National Institute for Occupational Safety and Health 2009. DHHS (NIOSH), 2009; Publication No. 125; Cincinnati, Ohio.
38. World Health Ogranization. Environmental Health Criteria Series; Kaolin and Selected Clay Minerals: Bentonite, 2005; No. 231.
39. Huang, Y. C.; Vieira, A.; Huang, K. L.; Yeh, M. K.; Chiang, C. H. J Biomed Mater Res A 2005, 75, 283.